

Supplementary Material

Intrinsic differences in spatiotemporal organization and stromal cell interactions between isogenic lung cancer cells of epithelial and mesenchymal phenotypes revealed by high-dimensional single-cell analysis of heterotypic 3D spheroid models

Maria L. Lotsberg^{1,2,3}, Gro V. Røsland^{1,2}, Austin J. Rayford^{1,2,4}, Sissel E. Dyrstad², Camilla T. Ekanger², Ning Lu^{1,2}, Kirstine Frantz⁵, Linda E. B. Stuhr², Henrik J. Ditzel^{5,6}, Jean Paul Thiery^{1,7,8}, Lars A. Akslen^{1,3,9}, James B. Lorens^{1,2} and Agnete S. T. Engelsen^{1,2*}

¹ Centre for Cancer Biomarkers (CCBIO), Department of Clinical Medicine, Faculty of Medicine, University of Bergen, Bergen, Norway

² Department of Biomedicine, Faculty of Medicine, University of Bergen, Bergen, Norway

³ Department of Pathology, Haukeland University Hospital, Bergen, Norway

⁴ BerGenBio, Bergen, Norway

⁵ Institute of Molecular Medicine, University of Southern Denmark, Odense, Denmark

⁶ Department of Oncology, Odense University Hospital, Odense, Denmark

⁷ Guangzhou Laboratory, Guangzhou, China

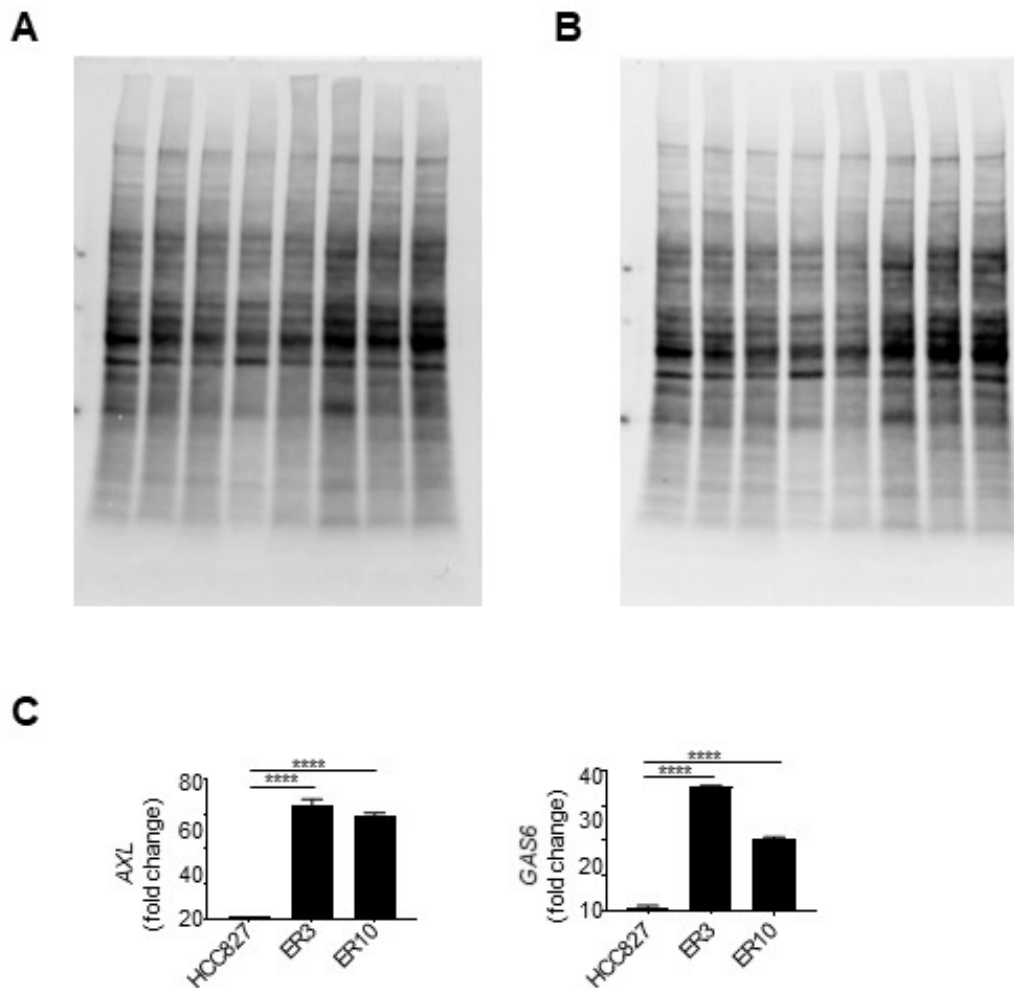
⁸ Gustave Roussy Cancer Campus, UMR 1186, Inserm, Université Paris-Saclay, Villejuif, France

⁹ Department of Clinical Medicine, Section for Pathology, Faculty of Medicine, University of Bergen, Bergen, Norway

* Correspondence: Dr. Agnete S. T. Engelsen E-mail: agnete.engelsen@uib.no

1 Supplementary Figures

Figure S1

**Figure S1: Total protein images for Western Blot quantification**

Total protein images used for quantification of Western Blot in Figure 1C, quantified in Figure 1D and 1F. Total protein for CDH1 (E-cadherin) and VIM (vimentin) blot is shown in (A) and CDH2 (N-cadherin) (B). (C) Expression of transcripts encoding *AXL*, and *GAS6*, assessed by RT-qPCR on cDNA prepared from HCC827 parental, ER3, and ER10 cells. RT-qPCR analyses were repeated $n = 3$ times, and representative results from one experiment with $n = 3$ technical replicates are presented in the figure as mean fold change \pm SD calculated by the $2^{-\Delta\Delta C_t}$ method. Two-way ANOVA followed by Tukey's multiple comparison test comparing ER3 and ER10 against the parental cell line was used to calculate statistical significance.

Figure S2

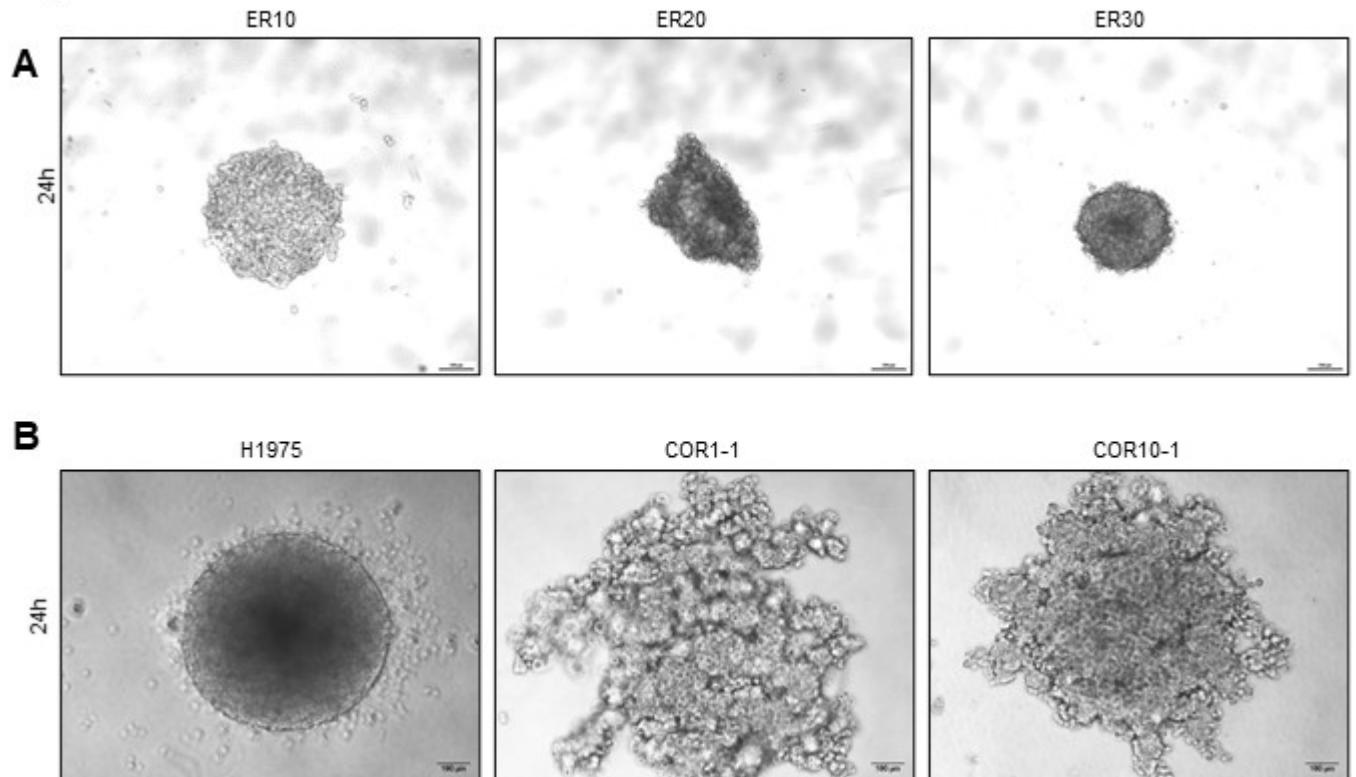


Figure S2: Spheroid formation in HCC827, COR1-1, COR10-1, ER10, ER20, and ER30.

(A) Nikon TE2000 images of ER10, ER20, and ER30 monoculture spheroids. Images were taken after 24 h using 4x objective. **(B)** Nikon TE2000 images of H1975, COR1-1, and COR10-1 monoculture spheroids. Images were taken after 24 h. 10x objective.

Figure S3

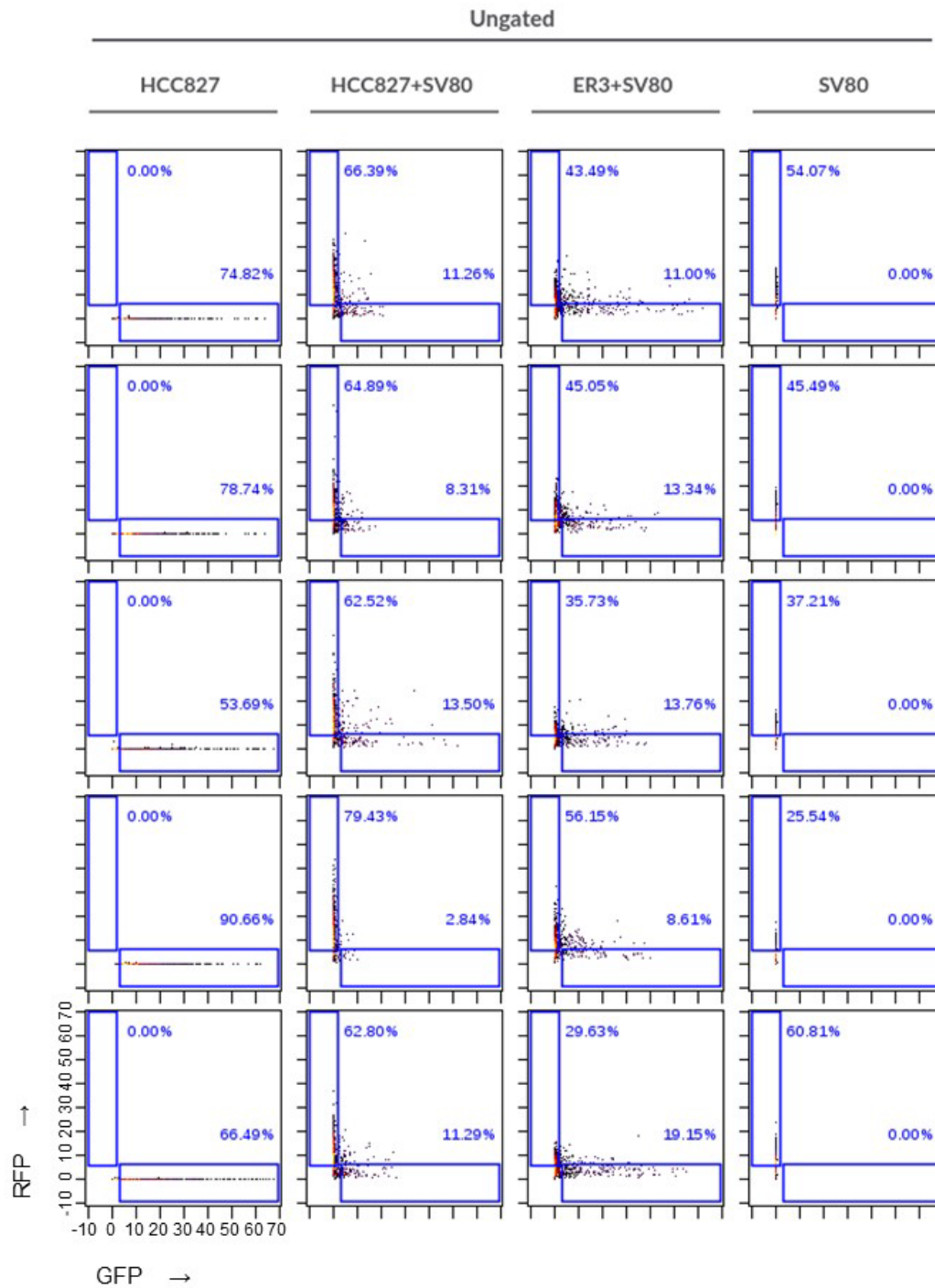


Figure S3: GFP+ and RFP+ gating strategy for untreated spheroids

Gating of GFP+ and RFP+ single-positive populations from the single-cell IMC data of untreated samples before visualizing channel intensities in the heatmap in Figure 7 Figure S4.

Figure S4

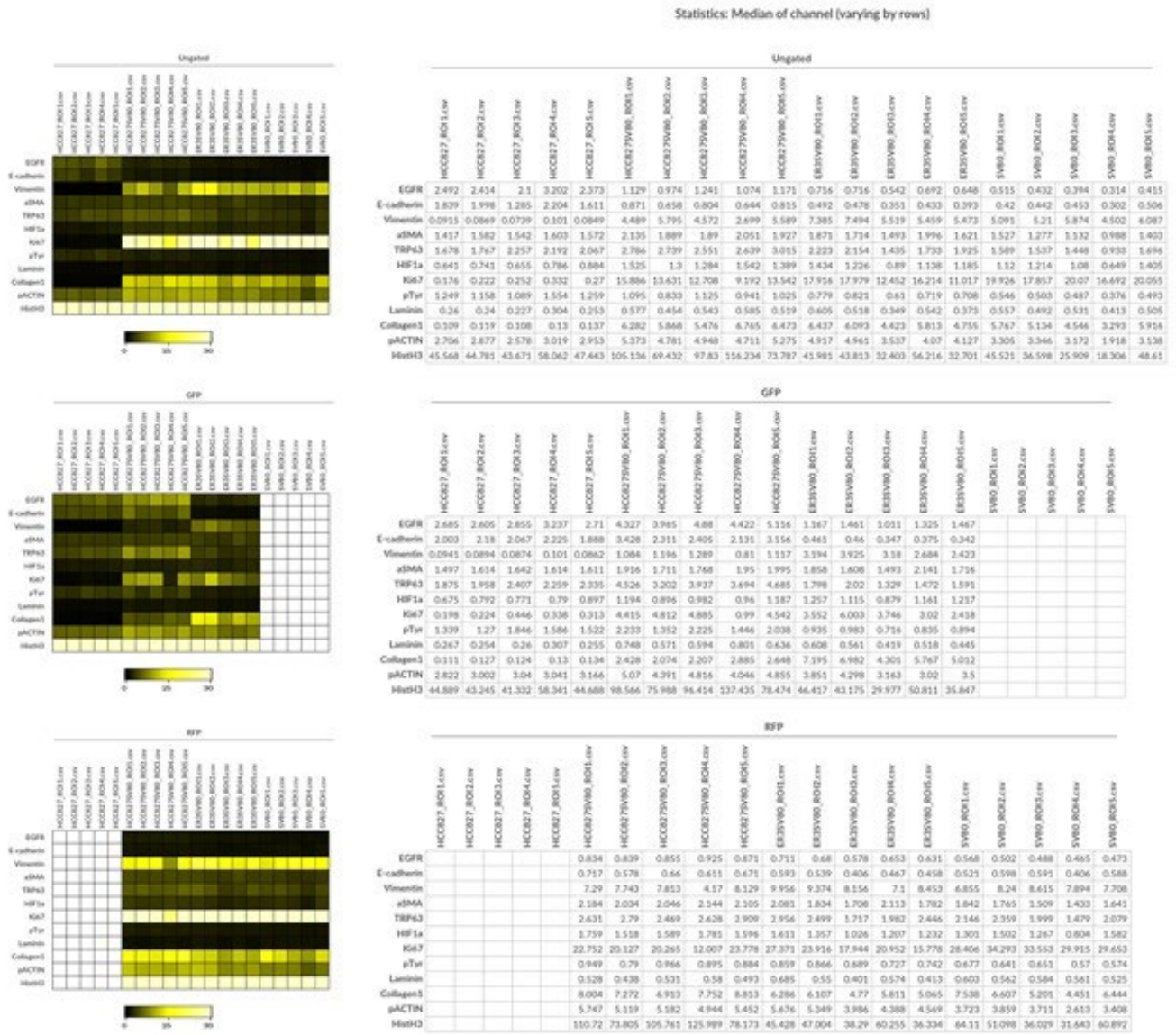


Figure S4: Heatmaps of channel expression in untreated spheroids

Median fluorescence intensity values and heatmap visualization for the untreated, GFP+ and RFP+ populations of the untreated samples.

Figure S5

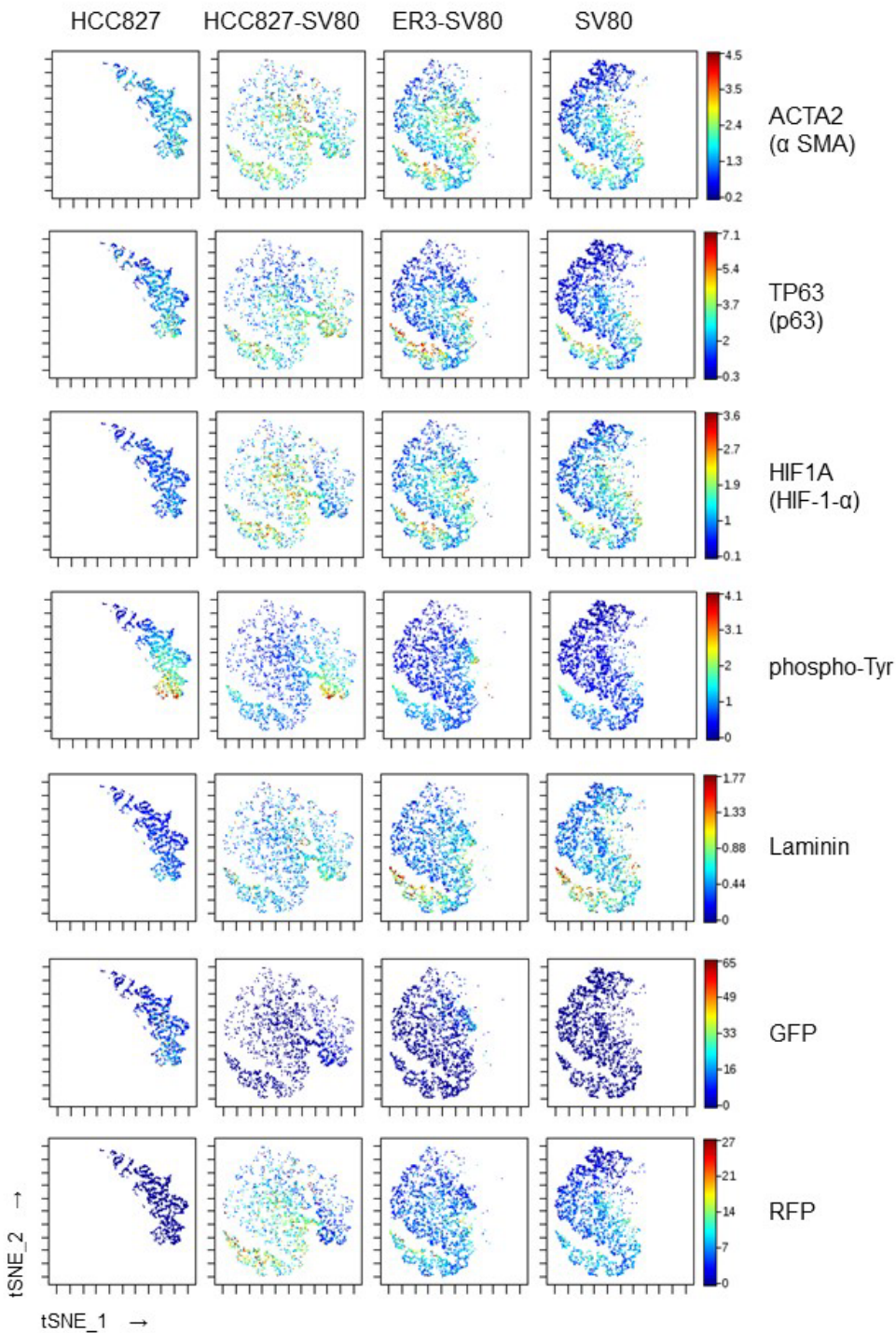


Figure S5: viSNE marker expression in untreated spheroids

Marker expression of ACTA2 (α SMA), TP63 (p63), HIF1A (HIF1 α), phosphor-Tyr, Laminin, GFP, and RFP displayed on the viSNE plots from untreated samples.

Figure S6

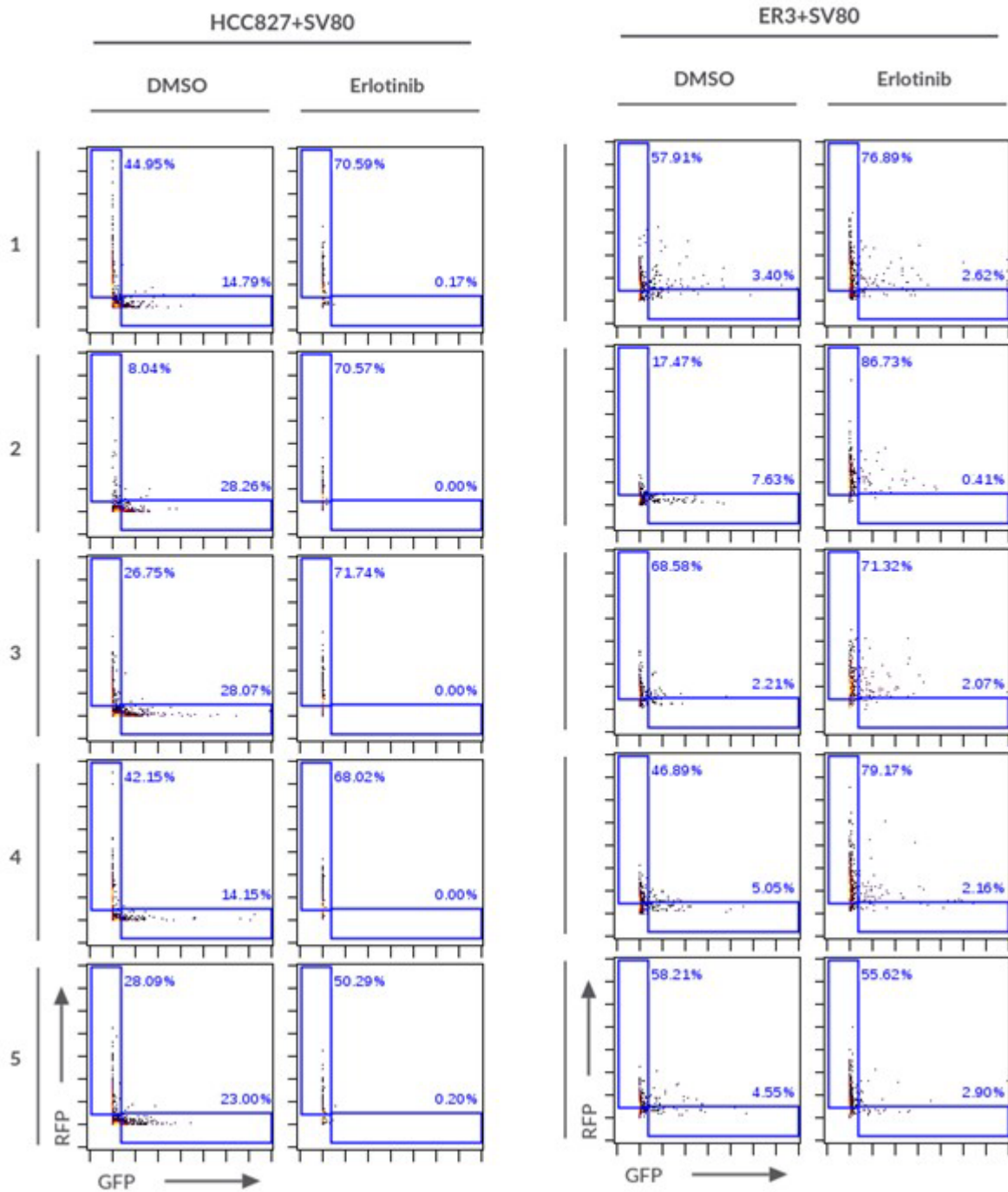
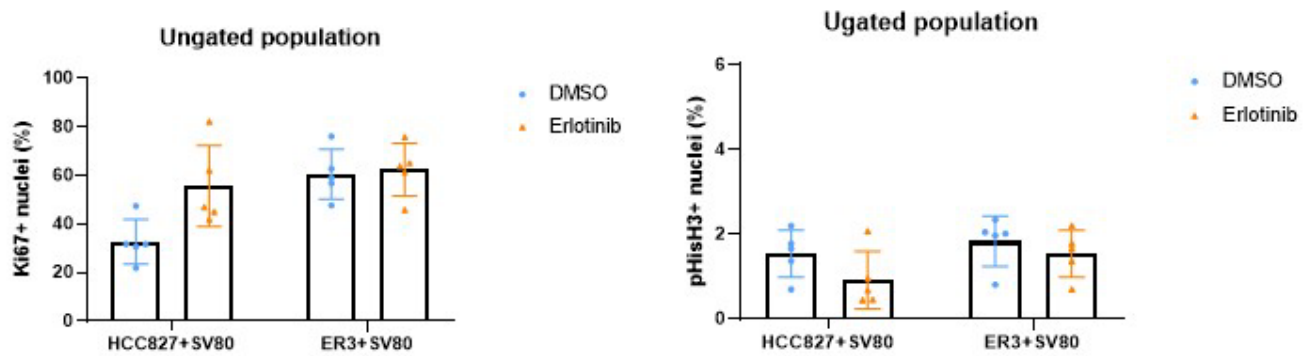


Figure S6: GFP+ and RFP+ gating strategy for treated spheroids

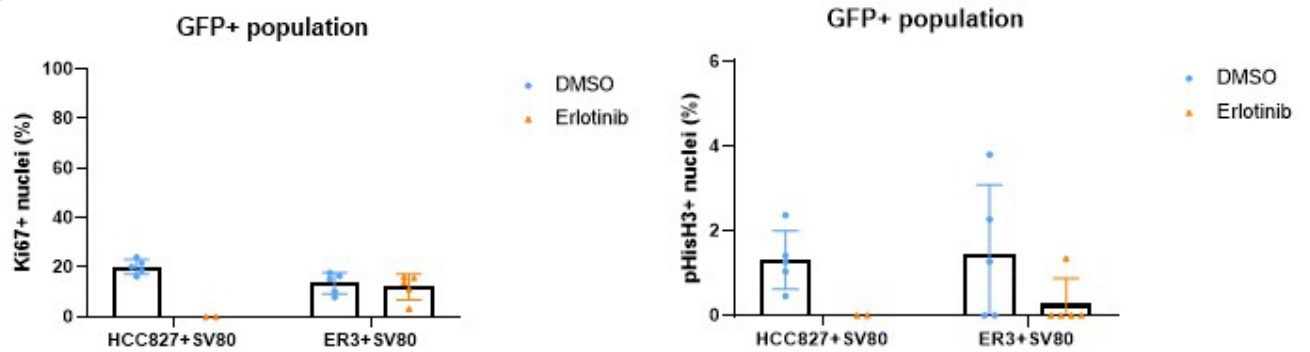
Gating of GFP+ and RFP+ single-positive populations from the single-cell IMC data from the DMSO and vehicle treated samples.

Figure S7

A



B



C

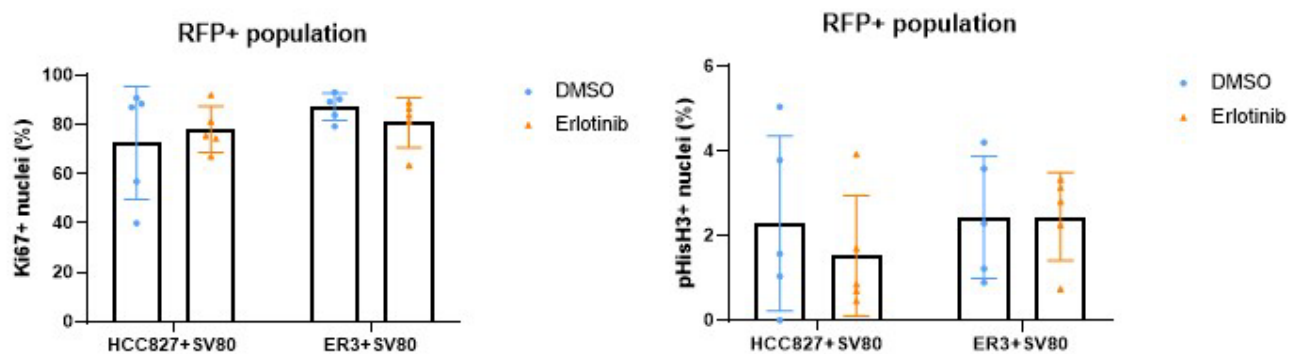


Figure S7: Percentage of Ki67 (MKI67) and phospho Histone H3 positive nuclei in vehicle (DMSO) and EGFRi (erlotinib) treated spheroids

Percentage of MKI67 (Ki67) positive (left) and phosphor-Histone H3 (pHisH3) positive (right) nuclei in the ungated (A), GFP+ (B) and RFP+ (C) populations of vehicle (DMSO) and EGFRi (erlotinib) treated spheroids. No statistical significance was found by the Mann-Whitney U-test using cytoBank to calculate the statistics.

Figure S8

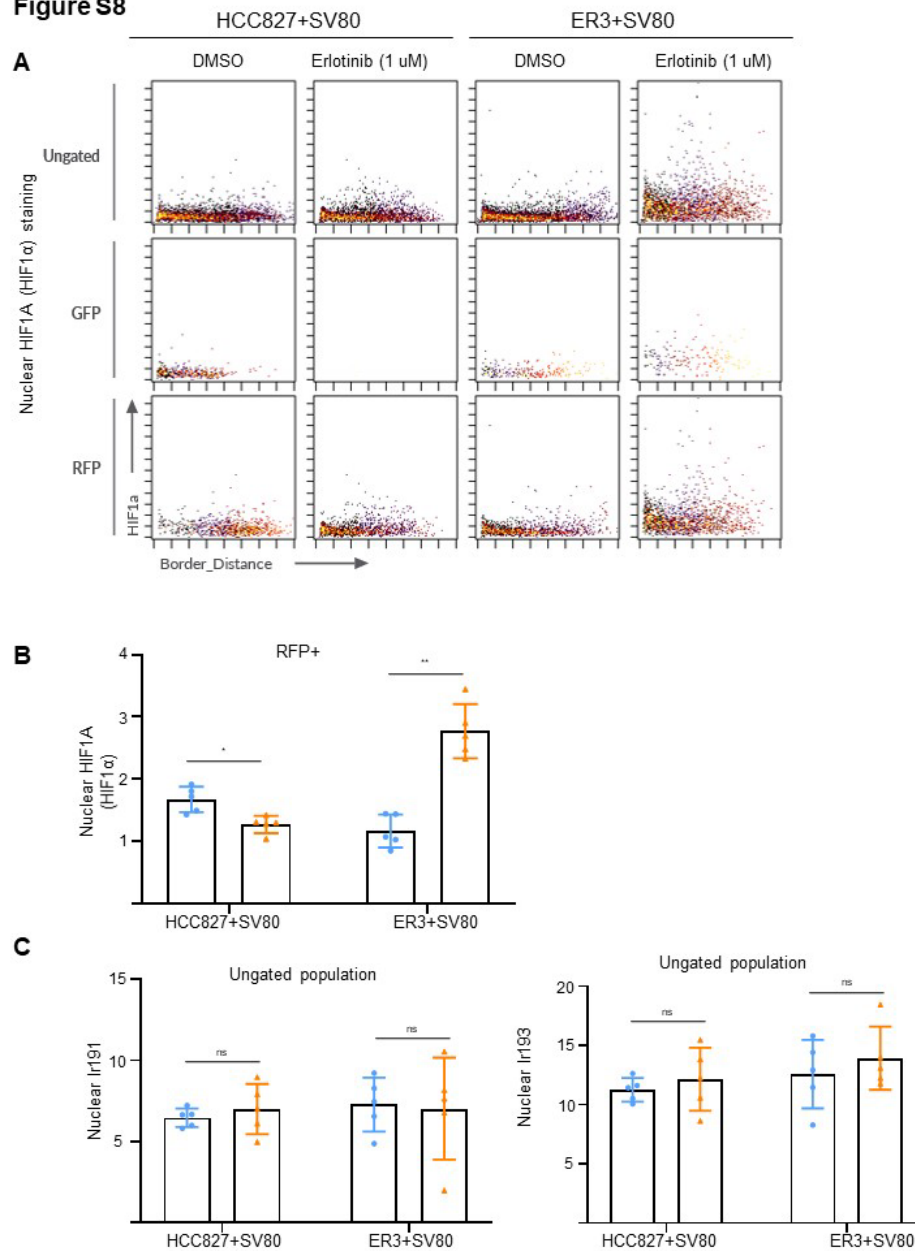


Figure S8: Scatter blots and channel expression of selected markers

- (A) Scatter plots displaying nuclear expression (mean channel intensity within the nuclei mask) of HIF1A (HIF1 α) plotted against distance to border in the ungated, GFP+ and RFP+ populations.
- (B) Bar chart displaying quantified nuclear HIF1A (HIF1 α) expression in the RFP+ population. Statistical significance in channel expression were calculated in cytobank using the Mann-Whitney U-test.
- (C) Bar charts displaying the nuclear Ir191 (left) and Ir193 (right) expression in the ungated populations of erlotinib and DMSO treated samples. No statistical significance was found by the Mann-Whitney U-test using cytobank to calculate the statistics.

Figure S9

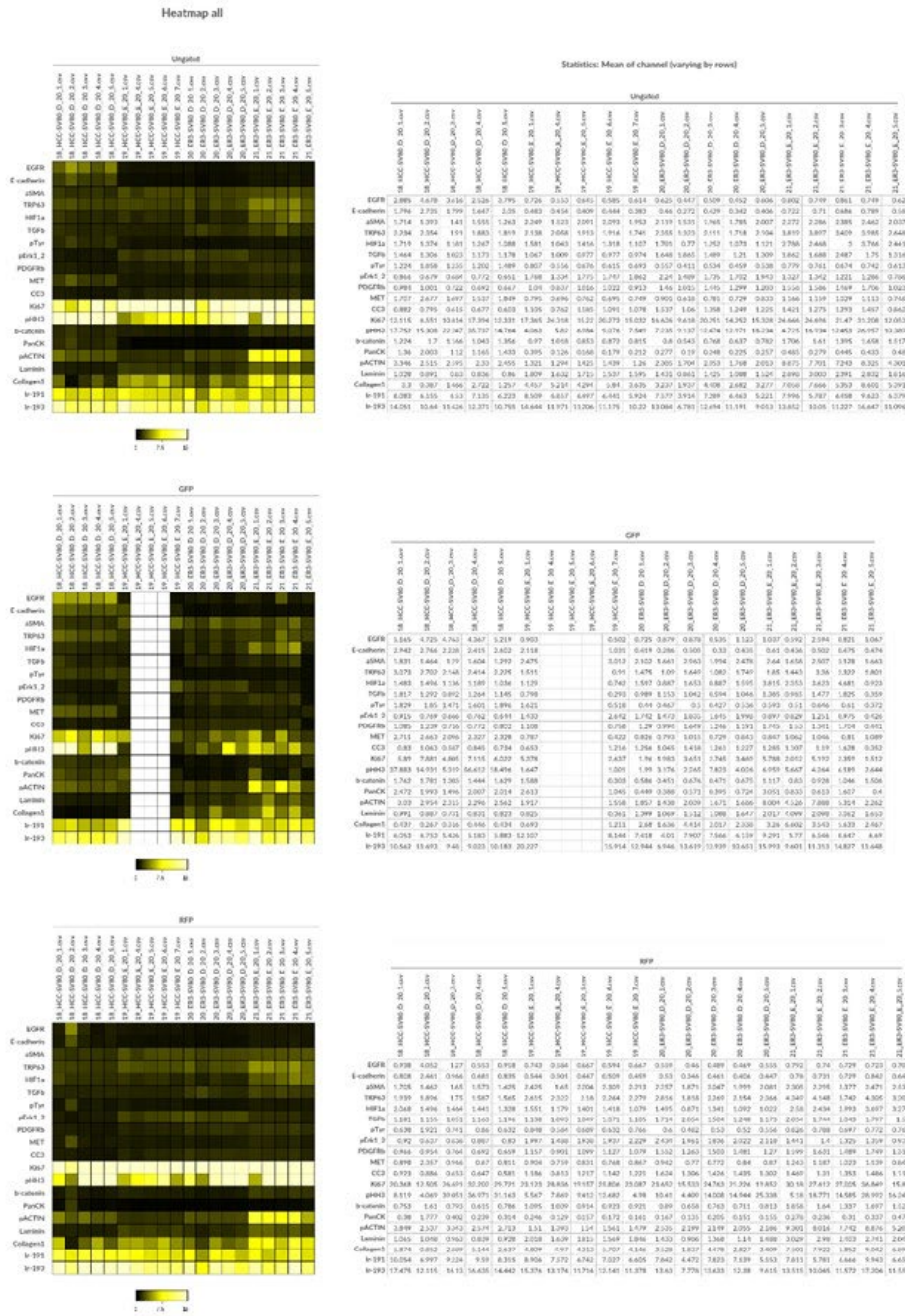


Figure S9: Heatmaps of marker expression of treated samples

Median fluorescence intensity values and heatmap visualization for the ungated, GFP+ and RFP+ populations of the vehicle (DMSO, D) and erlotinib (E) treated samples.

Figure S10

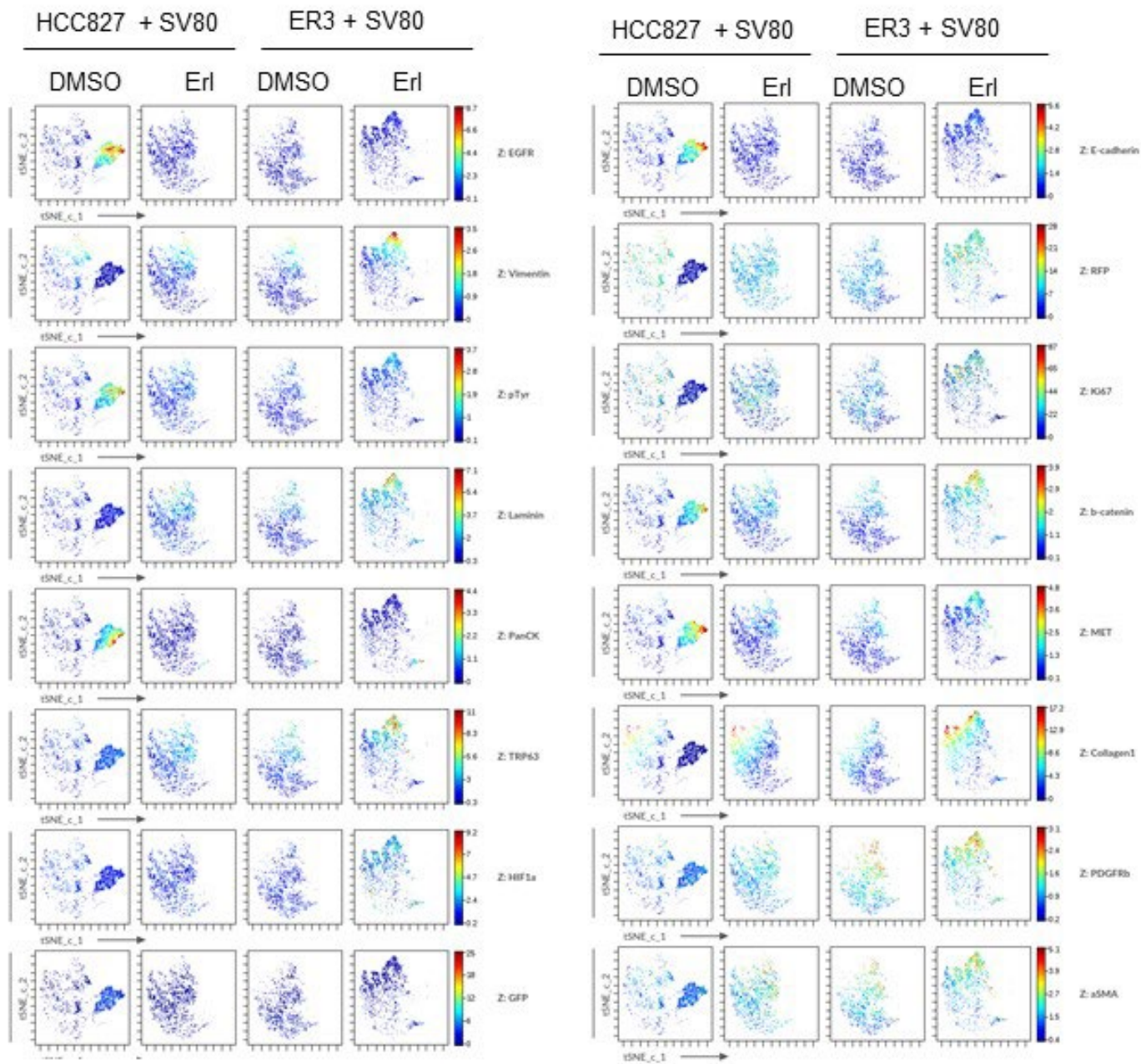


Figure S10: ViSNE marker expression of treated samples

Marker expression displayed on the viSNE plots for erlotinib and vehicle control (DMSO) treated samples.

2 Supplementary Videos

Video S1:

IncuCyte formation assay of ER3-GFP spheroids.

Video S2:

IncuCyte formation assay of SV80-dsRed spheroids.

Video S3:

IncuCyte formation assay of ER3-GFP + SV80-dsRed heterotypic co-culture spheroids.

Video S4:

3D reconstruction in IMARIS of ER3-GFP + SV80-dsRed heterotypic co-culture spheroids imaged by Zeiss confocal microscopy and counterstained with Hoechst nuclear dye.